COMITATO NAZIONALE PER L'ENERGIA NUCLEARE
Laboratori Nazionali di Frascati

LNF - 66/68
20 Dicembre 1966

R. Giantin, M. Grilli, M. Nigro, E. Schiavuta, P. Spillantini, F. Soso and V. Valente : POSITIVE PION PHOTOPRODUCTION WITH COHERENT BREMSSTRAHLUNG.
I: EXPERIMENTAL METHOD AND RESULTS. -

(Nota interna: n. 343)

Servizio Documentazione
dei Laboratori Nazionali di Frascati del CNEN
Casella Postale 70 - Frascati (Roma)

Laboratori Nazionali di Frascati del CNEN
Servizio Documentazione

LNF-66/68

Nota Interna: n. 343
20 Dicembre 1966

R. Giantin(x), M. Grilli, M. Nigro(x), E. Schiavuta(x), P. Spillantini, F. Soso, V. Valente(x): POSITIVE PION PHOTOPRODUCTION WITH COHERENT BREMSSTRAHLUNG.
I : EXPERIMENTAL METHOD AND RESULTS.

SUMMARY. -

The apparatus and the experimental method used for the measurements of the single π^+ photoproduction by linearly polarized γ rays is described. The present results on the asymmetry ratio $A(\theta)$ are summarized. The range covered by our results is $\theta = 30^o \div 145^o$(C.M.) and E_γ = 200 - 450 MeV.

(x) - Istituto di Fisica di Padova e I.N.F.N., Sezione di Padova.

INTRODUCTION. -

Linearly polarized photon beams make it possible to study some aspects of positive pions photoproduction that are not explicitly revealed in experiments involving unpolarized photons. In particular, the quantities $\sigma_\perp(\theta)$ and $\sigma_\parallel(\theta)$ can be determined separately, where $\sigma_\perp(\theta)$ ($\sigma_\parallel(\theta)$) is the differential cross section for producing a pion in a plane perpendicular (parallel) to the polarization plane of the incident photon. As the "retardation term" in π^+ photoproduction contributes only to $\sigma_\parallel$, the $\sigma_\perp$ is particularly suitable for a phenomenological theoretical analysis of the photoproduction process.

The complementarity of measurements by polarized and unpolarized γ'rays has been extensively discussed in many theoretical[1, 2, 3, 4] and experimental papers[5].

The experiment described below consisted of a measurement of the asimmetry ratio $A(\theta) = \sigma_\perp(\theta) - \sigma_\parallel(\theta) / \sigma_\perp(\theta) + \sigma_\parallel(\theta)$ as a function of pion angle (C. M.) ($\theta = 30^\circ \div 145^\circ$) for several photon energy ($E_\gamma = 200 \div 450$ MeV), for the process:

(1) $$\gamma + p = n + \pi^+$$

Part of the results of these measurements has been previously published; precisely that for $E_\gamma = 200 - 250$ MeV[6], and at $\theta = 90^\circ$ for $E_\gamma = 200 - 450$ MeV. In the present work we report more details on the features of γ's polarized beam (§ 1), on the apparatus (§ 2) and on the logic of the experiment (§ 3).

In part 4 we give, finally, a summary of the results. A very short discussion of these results is given in § 5. A full discussion on these data in comparison with the theoreticals prevision will be done later.

§ 1 - CHARACTERISTICS OF THE BEAM. -

The polarized γ'ray's beam was produced by the interaction of 1 GeV - electrons, of the Frascati electronsynchrotron, in a single diamond crystal by means of the well known process of coherent bremsstrahlung. This phenomenon was treated theoretically by Uberall[8] for the case of a two dimensional crystal. The experimental aspects, containing some qualitative features differing from the Uberall theory due to three dimensional nature of real crystals, has been observed and described by G. Barbiellini, G. Bologna, G. Diambrini and G. P. Murtas[9]. Their efforts have resulted in a linearly polarized photon beam available for use in experiments at the Frascati electronsynchrotron.

The characteristics of the beam are determined by the angle Θ between the incident electron direction, $\bar{p}_e$, and the (110) axis of the crystal and by the angle Φ between the planes (p_e, [110] and ([110] , [001]).

As is known, in comparison to the bremsstrahlung beam from an amorphous target there is an enhancement of the intensity in the neighborhond of certain γ ray's energies. The position (E_{peak}) of the "principal" maximum (the first maximum) can be varied by suitable adjustment of the angle Θ. In the region of this maximum the γ rays are linearly polarized.

Typical theoretical intensity and polarization curves are shown in fig. 1.

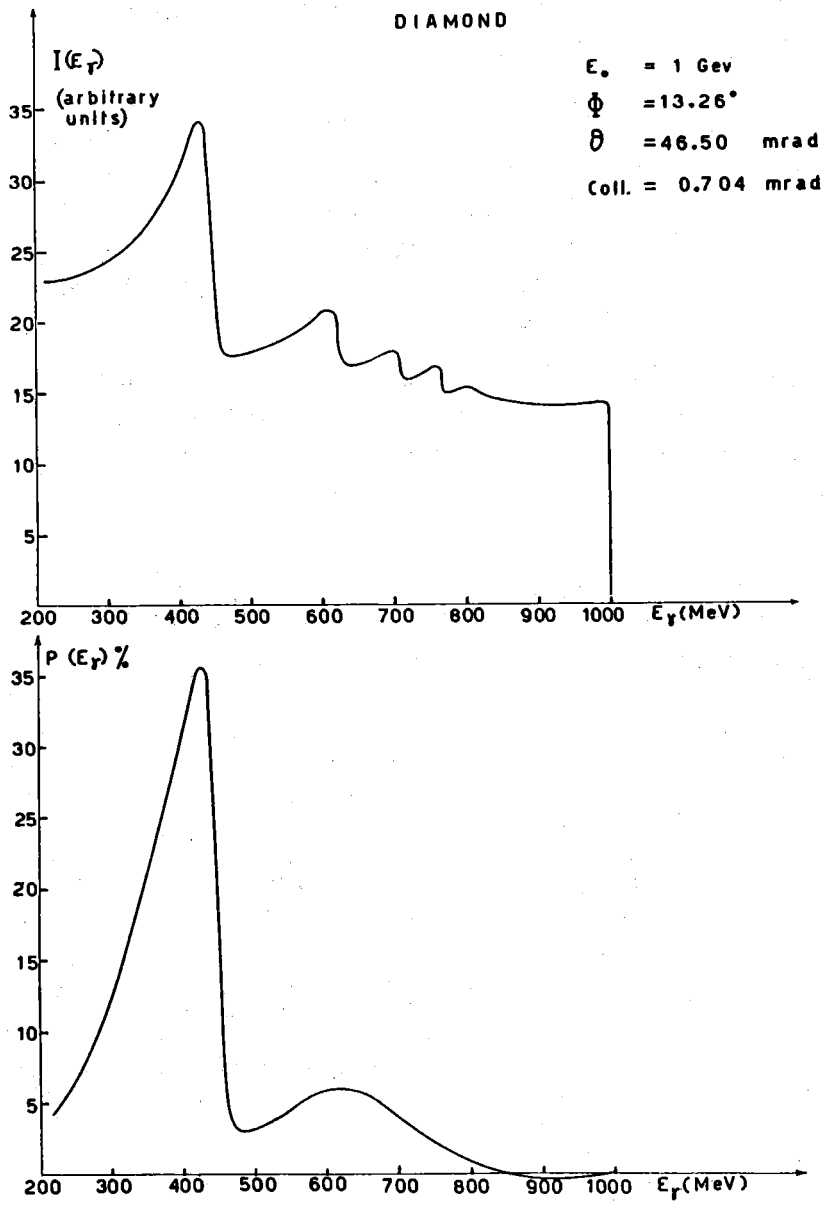

FIG. 1 - A theoretical intensity and polarization spectra in the case of coherent bremsstrahlung from 1 GeV electrons in a single diamond crystal.

In the following we will not discuss the features of such spectra but essentially the procedure and some precautions to use in order to work with a coherent beam, which involves several peculiar difficulties.

1) - Geometrical alignment of the crystal. -

During this operation great care has been applied in order to shield against possible sources of incoherent radiation from the crystal support, as these sources would reduce the coherence of the accepted spectrum.

2) - Search of "zero position" of the crystal. -

The search of the "zero position" of the crystal, i. e. the position $\phi = \theta = 0$, is a very critical operation because an error $\Delta\theta = 1'$ would shift E peak by ~ 4 MeV, which a similar error on θ or ϕ would give a variation of photon's intensity in the accepted energy band of $\sim 2\%$ (the corresponding polarization would vary by less than 0,01).

The "zero position" of the crystal was determined(x) by searching a minimum on the number of photons contained in a narrow energy band (fig. 2). The precision obtainable on the "zero position" is of the order of $\Delta\phi = \Delta\theta = \pm 0,5'$.

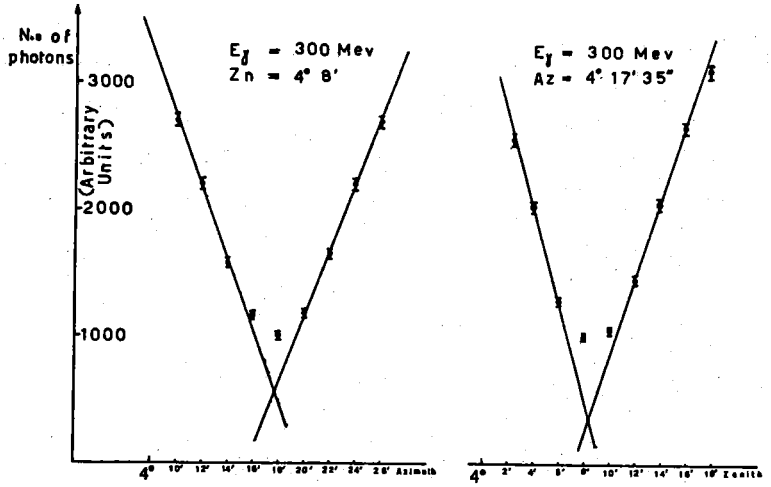

FIG. 2 - An example of the procedure to follow for searching the "zero position" of the crystal.

(x) - The (θ, ϕ) alignment was obtained by means of a remote control system and the goniometer connected to the crystal's support was wieved by a closed circuit television system.

3) - The intensity spectrum and the polarization of the beam. -

Actually the precision we obtained on photon's intensity was better than that corresponding to the indicated precision on "zero position" (see fig. 2). In fact, the photon intensity spectrum was measured contemporaneously with great detail, during the π^+ measurements by means of a pair spectrometer, (see fig. 4) and was required to reproduce accurately (within 0,3%) the exprected spectrum (see fig. 3).

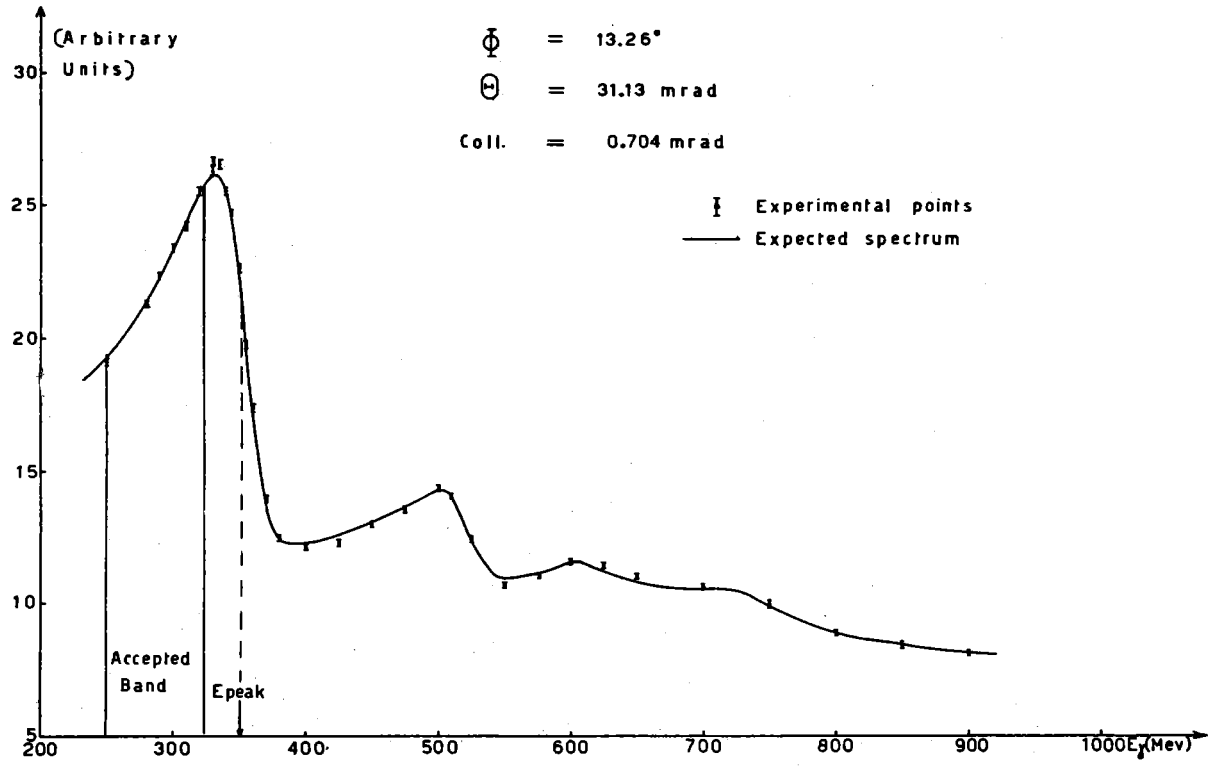

FIG. 3 - Comparison between a measured and the expected intensity spectrum.

This spectrum has been obtained(+) from the theoretical spectrum (see fig. 1) by including the following effects:

a) angular divergence of the primary beam of the electrons
b) multiple scattering of the electrons into the crystal
c) angular divergence of photon's beam (about 0,6 mrad in our experiment)
d) finite resolution of pair spectrometer ($\Delta E_\gamma / E_\gamma = \pm 4\%$).

The agreement required between the measured and expected spectrum limits the error in the polarization(x), calculated with the same procedure(+),

---

(+) - G. Bologna (private communication): more details on these calculations will be found in a next paper by this author on this subject.
(x) - For the definition of this quantity see (4) in § 3.

to less than $\Delta P = \pm 0,005$. By combining this precision with possible errors coming from crystal's alignment we estimate a total error in P certainly smaller than $\Delta P = \pm 0,01$.

Experimental checks of these calculations on P has been done at Frascati[10], or are in progress in this Laboratory[11] and at DESY[30]

§ 2 - EXPERIMENTAL APPARATUS. -

2.1. A general wiev of all the experimental apparatus is reported in figure 4.

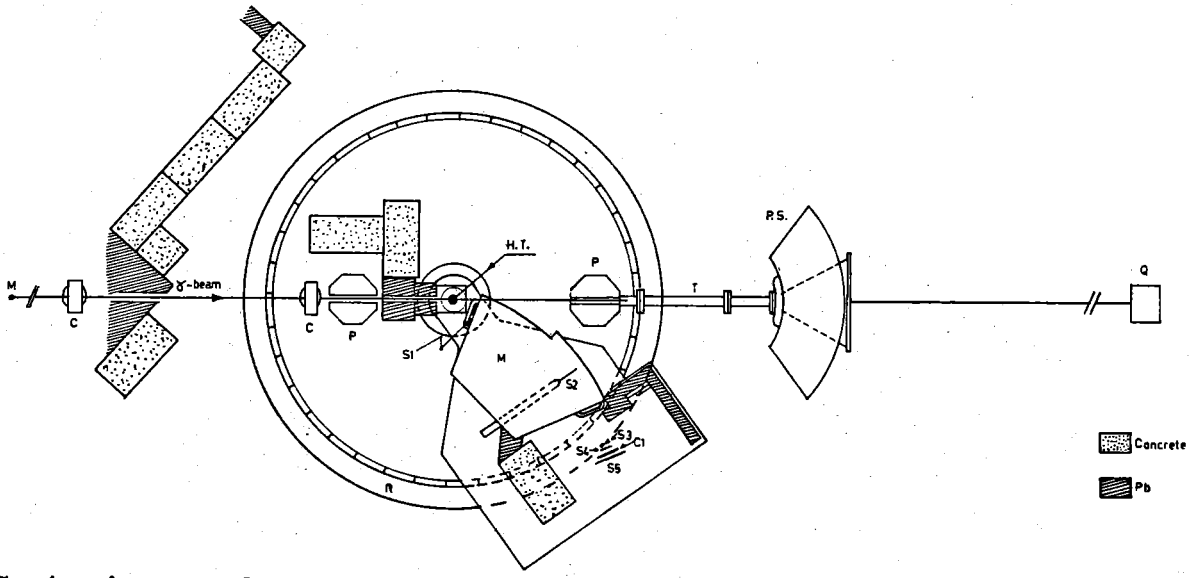

FIG. 4 - A general view of experimental apparatus: C = collimators; P = swipping magnet; H. T. = liquid hydrogen target; M = Magnetic spectrometer; P. S. = pair spectrometer; Q = quantameter (Wilson's type); $S_1 \ldots S_5$ = = plastic scintillators; C_1 = Cerenkov counter.

Positive pions, produced at a certain angle θ_L (LAB) were detected and identified by a system consisting of a strong focusing magnet and a counter telescope (see fig. 5).

The magnet has been extensively described by (12) (13). The principal characteristics of it are summarized in table I. The total momentum acceptance was $\Delta p/p = 0.25$ with a slowly varying solid angle over that region of acceptance of about $5 \cdot 10^{-3}$ sterad. By means of a three units counter system (A. B. C. in fig. 6) located in the focal plane the total momentum acceptance was divided in eight momentum channels.

Standard techniques were used to select the pions among the others particles. Protons did not have sufficient range to reach S_4. The electrons entering the spectrometer were largely eliminated by either or both of two

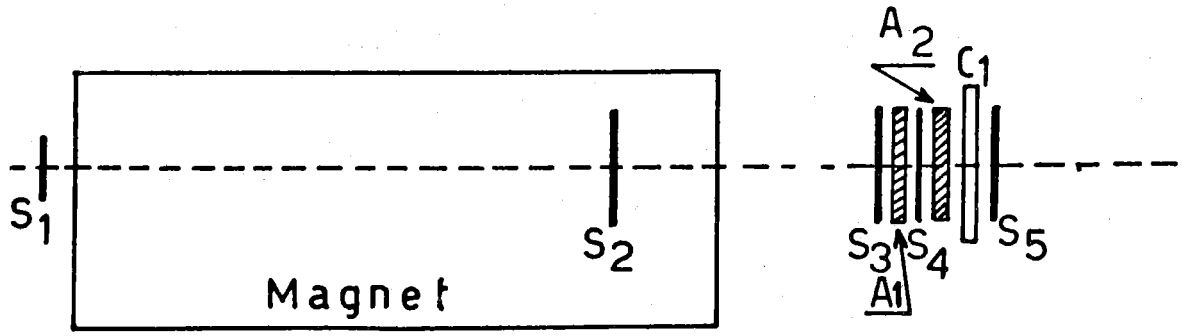

Fig. 5.1

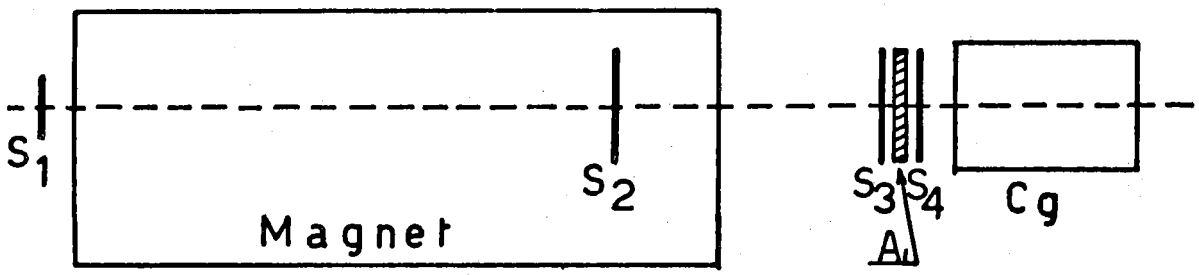

Fig. 5.2

$S_1,..,S_5$: Plastic Scintillators

C_1 : Plexiglass Čerenkov

Cg : Gas Čerenkov (CO_2)

$A_{1,2}$: Absorber (Cu)

FIG. 5 - Counter's telescope (not in scale)
5.1 - Telescope for "low" energy pions ($p < 200$ MeV/c)
5.2 - Telescope for "high" energy pions ($p > 200$ MeV/c)

veto counters: the water Cerenkov C_1 (see fig. 5.1), in which electrons but not pions would produce Cerenkov radiation, and S_5 that would be reached by surviving electrons while the pions stopped, for $p < 200$ MeV/c ("Low energy pions"), in the absorber A_2. In the measurements of π with higher momentum ($p > 200$ MeV/c) (see fig. 5.2) we have used a gas Cerenkov counter [C_g; CO_2; 5-7 Atm] to reject the electrons. In either cases the rejection efficiency against the electrons was $\sim$ 95%.

TABLE I - Parameters of the magnet.

Source-magnet distance	S_o	= 31 cm
Image-magnet distance	d	= 51.6 cm
Total distance source-image	S	= 261 cm
Linear magnification (horizontal)	M_H	= 0.2
Linear magnification (Vertical)	M_V	= 6
Dispersion (at the image position)	D	= 0.03 cm^{-1}

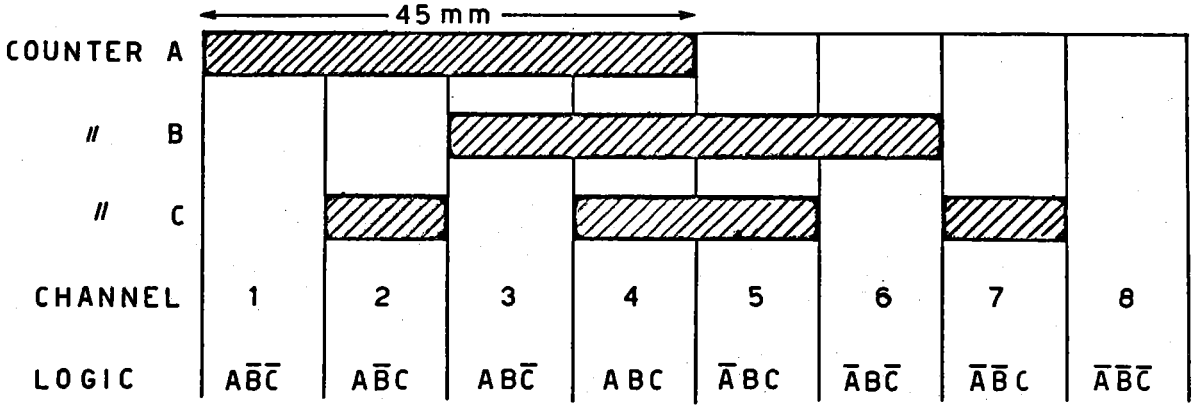

FIG. 6 - Eight momentum channels system. The tree counters A, B, C are indicated as a unique counter S_3 in fig. 5.

2.2. The block diagram of the system used to identify the π^+ (in the case $p > 200$ MeV/c) is shown in fig. 7.

A first coincidence

$$Q = S_1 S_2 S_3 S_4$$

defines particles (pions and electrons) of the correct momentum band, which traverse the telescope. The Cerenkov counter signal (gated by Q) in coincidence with Q (QC) or in anticoincidence ($Q\bar{C}$) separates the electrons from the pions. Figure 8 shows the efficiency curve of this counter.

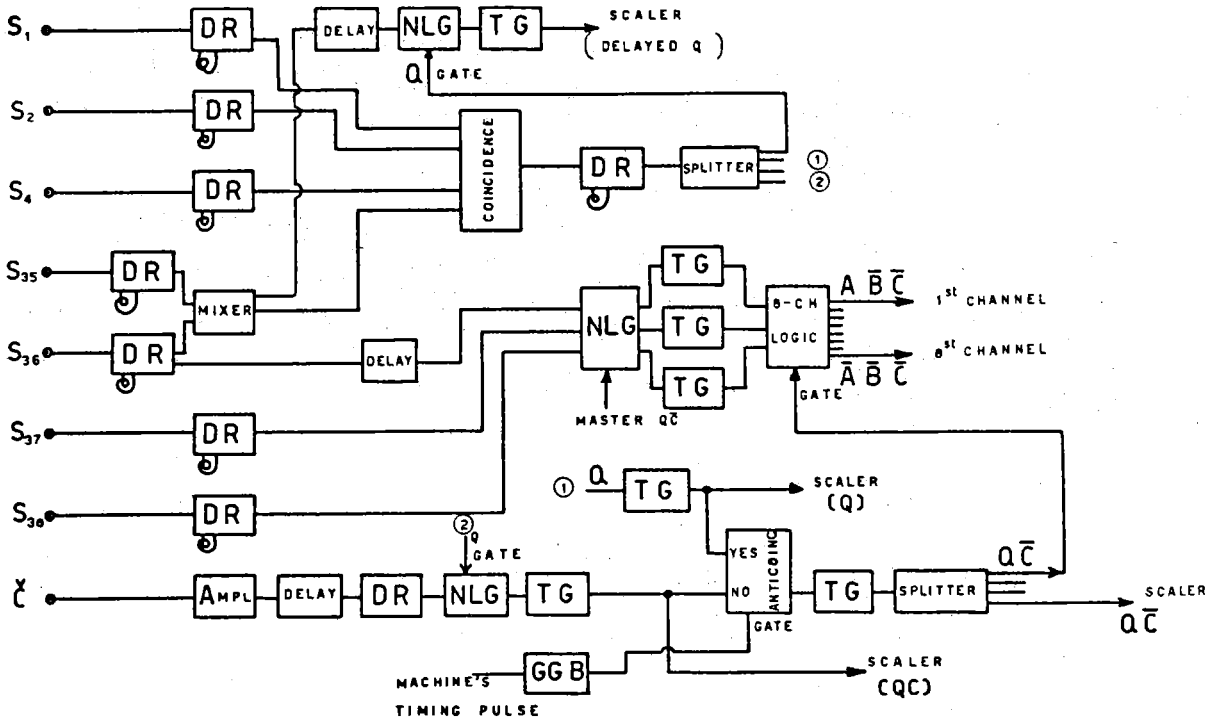

FIG. 7 - Electronics block diagram: AMP = amplifier; DR = Fast discriminator and shaper; NLG = Non linear gate; TG = Trigger; GGB = Beam-syncronized gate.

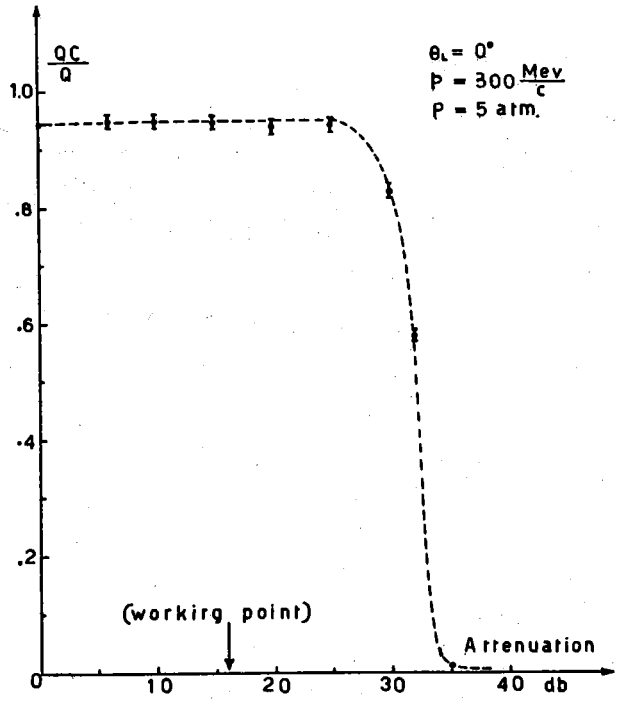

FIG. 8 - Efficiency curve for the gas Cerenkov. The measurement of this efficiency was made with the same geometry used during the experiment (beam's divergence at the Cerenkov $\delta \sim \pm 6^{o}$ (6). The efficiency of this Cerenkov for a "parallel" beam ($\delta = \pm 3^{o}$) of electrons was better than 99%.

The "master" $Q\bar{C}$ is used to gate the signals of the counters S_{36}, S_{37}, S_{38}. (A, B, C, respectively, in fig. 6). A 8 channel logic circuit (8-CH LOGIC in fig. 7) makes the correlations

$$\bar{A}\bar{B}\bar{C},\ \bar{A}\bar{B}C,\ A\bar{B}\bar{C},\ ABC,\ \bar{A}BC,\ \bar{A}B\bar{C},\ \bar{A}\bar{B}C,\ \bar{A}\bar{B}\bar{C}.$$

which correspond, respectively, to eight channels of increasing momentum.

In order to get a good stability of the counting apparatus we have worked with standardized pulses from each counter (see fig. 7) and the working condition of these counters has been periodically checked.

§ 3 - EXPERIMENTAL METHOD. -

3.1. We have measured the asimmetry ratio

$$(2) \qquad A(\theta, E_\gamma) = \frac{\sigma_\perp(\theta, E_\gamma) - \sigma_{\parallel}(\theta, E_\gamma)}{\sigma_\perp(\theta, E_\gamma) + \sigma_{\parallel}(\theta, E_\gamma)}$$

starting from the observed pion's yield (C_+, C_-) by means of the relation

$$(3) \qquad A(\theta, E_\gamma) = \frac{1}{P} \frac{C_+(\theta, E_\gamma) - B_+(\theta, E_\gamma) - C_-(\theta, E_\gamma) - B_-(\theta, E_\gamma)}{C_+(\theta, E_\gamma) - B_+(\theta, E_\gamma) + C_-(\theta, E_\gamma) - B_-(\theta, E_\gamma)}$$

where

$$(4) \qquad P = \frac{N_\perp - N_{\parallel}}{N_\perp + N_{\parallel}}$$

is the beam's polarization ($N_\perp$ ($N_{\parallel}$) is the relative number of photons having their electric vector perpendicular (parallel) to the (γ, π) plane). The quantities $\sigma_\perp(\theta, E_\gamma)$, $[\sigma_{\parallel}(\theta, E_\gamma)]$ has been previously defined (see "Introduction"). The other quantities entering (3) are:

$C_+(\theta, E_\gamma)$ $[C_-(\theta, E_\gamma)]$ total yield of pions, in the accepted momentum band and for a given angle θ, for a fixed number of incident photons in a narrow energy band around E_γ, when $P > 0$ ($P < 0$).

$B_+(\theta, E_\gamma)$ $[B-(\theta, E_\gamma)]$ background events in process (1), measured in the same conditions as the corresponding C_+ and C_-.

The kinematical conditions (E_γ, θ) were fixed by measuring the pions at a fixed angle and momentum in the lab. system ($\theta_{L,p}$).

The cross section $\sigma_\perp$ and $\sigma_{\parallel}$ are related to the observed counting rates as follows:

$$(5) \qquad C_{\pm} - B_{\pm} = K(\sigma_{\perp} N_{\perp} + \sigma_{\parallel} N_{\parallel}) = \frac{K}{2}(N_{\perp} + N_{\parallel})(\sigma_{\perp} + \sigma_{\parallel})\left[1 \pm |P| A\right]$$

where the proportionality constant K, depending on target size, solid angle, etc., is the same for the two sign of beam's polarization.

From the relation (5) we obtain (3) assuming that the absolute value of the polarization P, and the total number of photons in the accepted energy band, $(N_{\perp} + N_{\parallel})$, are the some for the two cases C_+ or C_-.

We have obtained, during the experiment, this equality of $|P|$ and of the photon's intensity by requiring that the two γ ray's intensity spectra simultaneously measured in the case $P > 0$ and $P < 0$ agree better than 0.5% (see fig. 9).

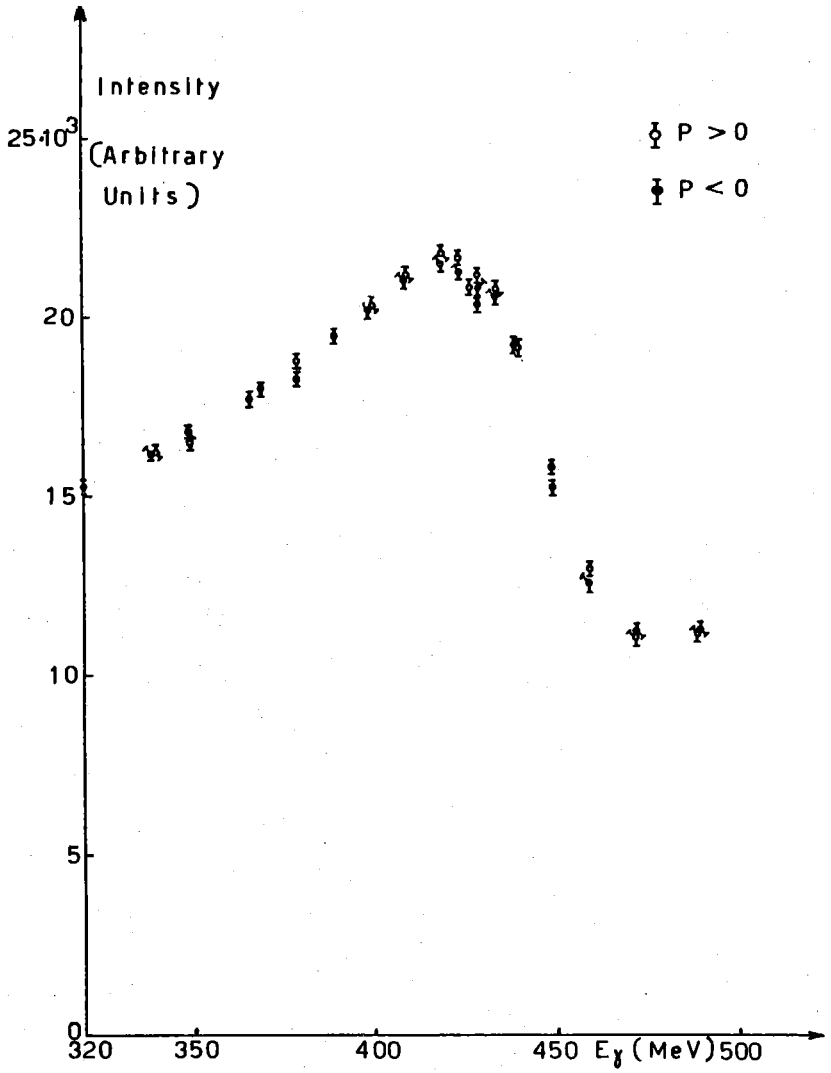

FIG. 9 - A comparison between two experimental intensity spectra relative to the cases $P \gtrless 0$.

Actually, during our measurements we have used, for experimental convenience, not a single diamond crystal but two different crystals in order to obtain the two sign of beam's polarization. Both the zero position and the photon's spectrum of these two crystals were accurately and countinuously checked, as we have said, by means of the pair spectrometer. These crystals could be inserted or taken out without any change in their zero position and so a very short time was needed for an accurate allignment. This fact allows us to interchange many times the two crystals during a run, and so to alternate the measurements of C_+ and C_-. This procedure results to be very useful in the measurements of small asimmetries (see fig. 10).

Moreover, during the elaboration of the data, a statistical analysis (χ^2 test) has been done of the $C_\pm$ yields of the different channels, in order to check their internal consistence.

3.2. The most important contribution to the background, i.e. to the B_+ (or B_-), comes from processes originating from higher energy photons, as the coherent bremsstrahlung beam extends until 1 BeV whereas the investigated interval producing single π^+ events is centered near to the "principal" maximum (see fig. 3). Hence two backgrounds are present: π's, with the right momentum and angle, due to multipion processes and muons from decay of higher energy π's before or inside the magnet.

The "multipion background" has been measured or estimated in different ways:

a) We have measured the pion's yield at a fixed kinematical condition (θ_L, p) for different values of the crystal's angle Θ, which means for different position (E_{peak}) of the "principal" maximum (§ 1).

This total yield is the superposition of a contribution of single π^+ events which varies rapidly when the principle peak of the bremsstrahlung spectrum is made to "sweep" the energy band accepted by the experimental arrangement, and a slowly varying contribution of multipion's processes originated by the high energy region of the bremsstrahlung spectrum. In fact the number of photons whose energy is above the kinematical threshold for double (or multi -) production varies very slowly with the angle Θ.

Thus we may write for the pion's yield

$$C_+(\theta, \theta_L, p) = C_+(\text{single}) + C_+(\text{multipion}) =$$

$$= K \left\{ \int_{\Delta E_\gamma \Delta \Omega_L} N(\theta, E_\gamma) \frac{d\sigma_s(\theta_L, E_\gamma)}{d\Omega_L} \left[1 + P(\theta, E_\gamma) \cdot A(\theta_L, E_\gamma) \right] \cdot G(E_\gamma)\, d\Omega_L\, dE_\gamma + B_+(\theta, \theta_L, p) \right\} \tag{6}$$

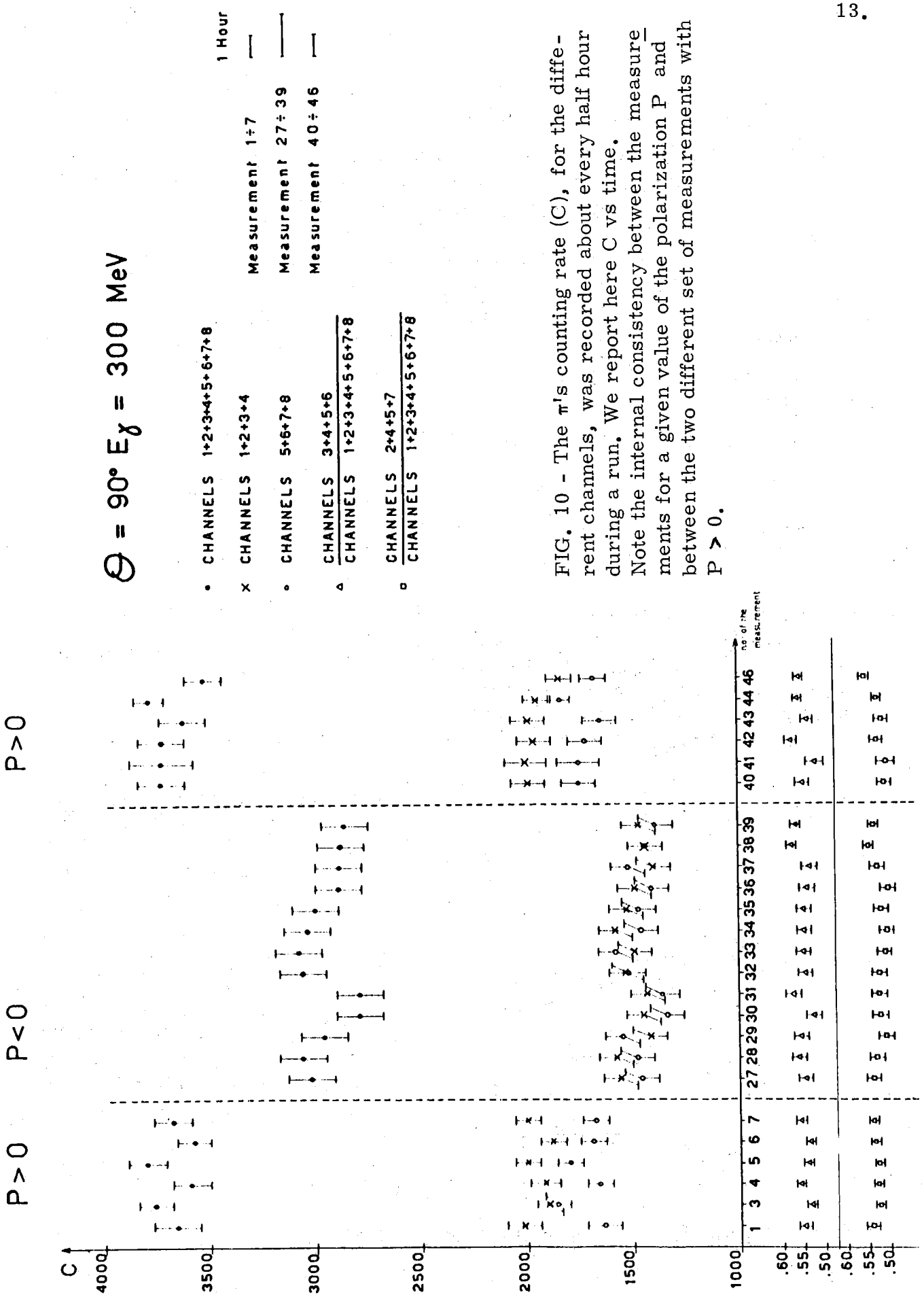

FIG. 10 - The π's counting rate (C), for the different channels, was recorded about every half hour during a run. We report here C vs time. Note the internal consistency between the measurements for a given value of the polarization P and between the two different set of measurements with P > 0.

The quantities entering in (6) are:

$N(\theta, E_\gamma)$: number of photons with energy E_γ when the crystal's angle is equal to Θ. This number is obtained from experimental spectra of the type reported in fig. 3.

$d\sigma s/d\Omega_L$: differential cross section for unpolarized photons of energy E_γ to produce a pion in a single photoproduction process. For this cross section we have used the results of ref. (14).

$G(E\gamma)$: energy resolution function of the apparatus.

ΔE_γ , $\Delta \Omega_L$: energy band and solid angle accepted.

The quantities K, P, and A have been defined in § 3.1. The subscripts (+) refers to photons with polarization $P > 0$.

The multipion background $B(\Theta; \theta_L, p)$ is given by

$$(7) \quad B(\Theta;\theta_L p)=\int_{\Delta E_\pi \Delta\Omega_L} \int_{E_{\gamma th}}^{E\gamma max} N(\Theta, E'\gamma)dE'\gamma \frac{d^2\sigma p}{d\Omega dE_\pi} G(E_\pi)d\Omega_L dE_\pi$$

when ΔE_π is the spread in pion energy corresponding to ΔE_γ in (6) and $d^2\sigma p/d\Omega dE_\pi$ the differential cross section by unpolarized photons of energy $E'_\gamma > E_\gamma$ threshold, to produce in a multipion process a π^+ at (θ_L, p) (where p is the momentum corresponding to the energy E_π). We have assumed that this contribution is the same for the two sign of beam's polarization, as for $E_\gamma > E_{\gamma th}$ the polarization is very low.

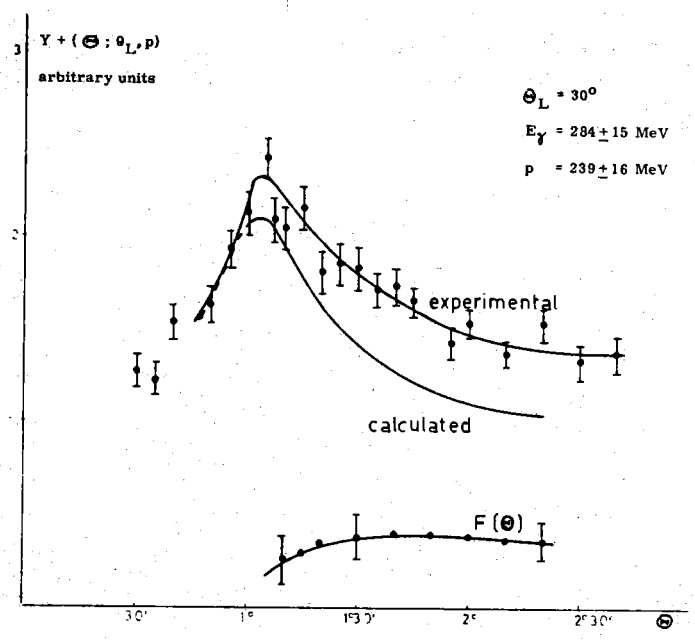

By comparison of the experimental "C vs Θ curve" with the theoretical one calculated from the first term of (6) it is possible to obtain the function F of the multipion background (see fig. 11).

As it was expected $B(\Theta)$ was found to be constant with Θ and its values for some typical kinematical conditions are summarized in table II. In this table the multipion background is expressed as percentage on the total pion's yield for the various experimental conditions, i.e. for the fixed Θ at which we measured the symmetry.

FIG. 11 - Y_+ vs Θ curve (see text § 3.2)

TABLE II - $B/[C_+(\text{single}) + C_+(\text{multipion})]$

θ_{cM} \ E_γ (MeV)	225	300	400
30°	.50±.10	.15±.05	.45±.10
45°	.23±.10	.12±.04	.30±.04
90°	.05±.05	.04±.05	.16±.06

The measured values of B are in agreement with numerical calculation of (7) in which $d^2\sigma p/d\Omega dE\pi$ is taken from the data of other Laboratories[16, 17].

b) Direct measurements of multipion contribution due to the process

(8) $$\gamma + p \rightarrow p + \pi^+ + \pi^-$$

have been performed revealing the π^- in the same kinematical condition as for π^+ in single photoproduction process and with the same coherent beam's spectrum, only reversing the current in the magnetic spectrometer.

From such measurements we have estimate the total multipion background, including the process (8')

(8') $$\gamma + p \rightarrow n + \pi^+ + \pi^o$$

making use of the experimental data of Bloch and Sand[16] and of Kusumagi et al.[17] to fixe the relative weight of the two processes.

Also these calculations agree with the results of table II.

Besides to the multipion background now discussed we have also some losses in the pion's counting rate due to the ($\pi \rightarrow \mu$) decay of pions of right momentum along their trajectories. As this loss is equal, for the two cases ($P \gtrless 0$), i.e. of the type $B_+/C_+ = B_-/C_-$, it can be ignored, in the calculation of the asymmetry A (see (2)). Moreover, because of the momentum discontinuity at the decay, we have contamination also from parent π's with a momentum outside our accepted band. A part of this contamination is contained in the multipion subctraction just discussed.

Finally, some other minor backgrounds (like empty target(x)) are also of the type $B_+/C_+ = B_-/C_-$ and, therefore, have been ignored in the calculation of A.

(x) - The empty target contribution has been measured for different kinematical conditions and resulted to be less than 5%.

§ 4 - With the technique and the procedure described in the preceding paragraphs we have measured the asimmetry ratios $A(\theta, E_\gamma)$, for $\theta = 30^o$, 45^o, 71^o, 90^o, 120^o, 133^o, 144^o and $E\gamma = 200 - 450$ MeV, reported in fig. 12. We are completing the measurements of $A(\theta, E\gamma)$ for the backward angles by means of a range telescope (without magnet).

As we have explicity shown in[7] (see fig. 1 in[7]) many measurements of $A(\theta, E_\gamma)$ have been repeated with different values of beam's polarization P and were found to be completely consistent.

The errors reported for A have been calculated by means of the following expression:

$$(9) \qquad \Delta A = \frac{2}{P} \frac{R}{(R+1)^2} \left\{ \left(\frac{C_+}{C_+ - B}\right)^2 + \left(\frac{C_-}{C_- - B}\right)^2 + h^2 \left(\frac{\Delta B}{B}\right)^2 + A^2 \left(\frac{\Delta P}{P}\right)^2 \right\}^{1/2}$$

where $R = \dfrac{C_+ - B}{C_- - B}$ and $h = \dfrac{(C_+ - C_-)/B}{\dfrac{C_+ C_-}{B^2} - \dfrac{C_+ - C_-}{B} + 1}$

The first two terms in (9) are the statistical errors of the yields C_+ and C_-, whereas the third and fourth therms are, respectively, the relative error on the background B and on the beam's polarization P.

The statistical errors in our experiment was $\sim (1 \div 2)\%$ ($C_+ \sim C_- \geq \geq 10,000$). The error in the beam's polarization was estimated to be $\Delta P/P \sim \sim 2\%$, so the therm $A \cdot (\Delta P/P)$ gives a contribution to ΔA of the same order of the statistical error.

The precision in the multipion background (see table II in 3.2.) is, generally, worse. But, the contribution of this background subtraction in ΔA is depressed, by the coefficient h which is, generally, much less than unity.

§ 5 - We report some indications on the methods we are following for the analysis of the data.

1) - Comparison between theory and experiment. -

The general trend of the experimental data for $A(\theta, E_\gamma)$, as shown in fig. 3(a, b) of reference (6) and in fig. 12, is reproduced by the previsions of more recent dispersive theories proposed for photoproduction process.

Neverthless we have no quantitative agreement between the measured and predicted values. These discrepances could be explained by revaluating the non resonant multipole amplitudes (E0+, M1-, E1+). In fact the asimmetry $A(\theta, E_\gamma)$ is particularly sensitive to such multipoles[18, 19, 20] which

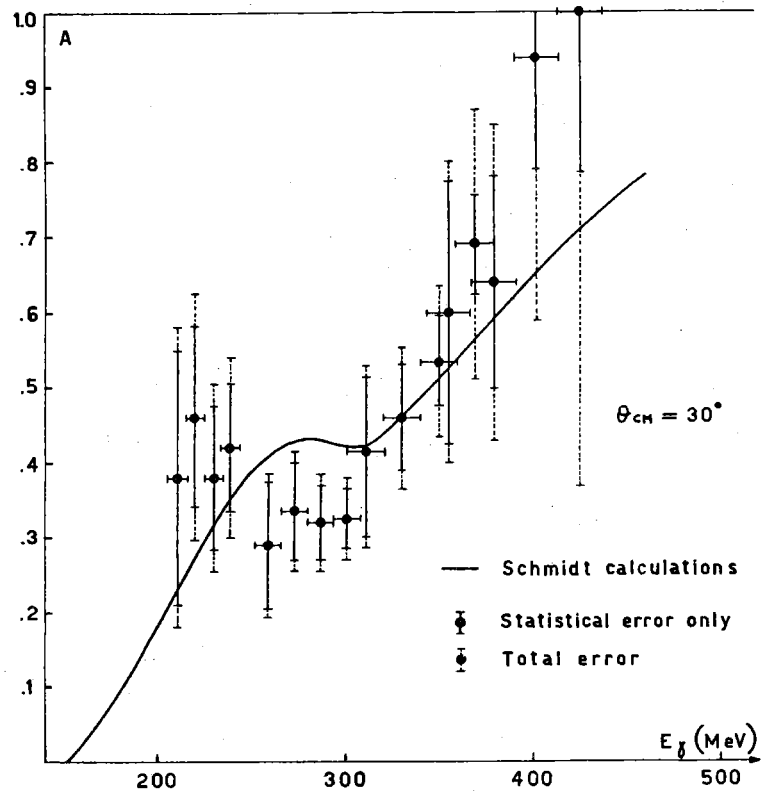

FIG. 12 a)

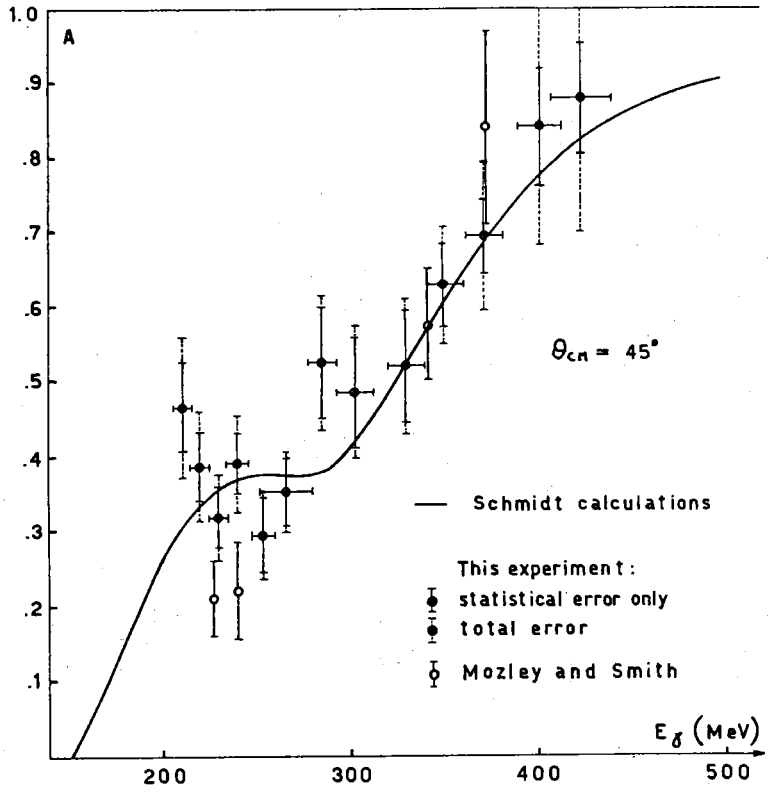

FIG. 12 b)

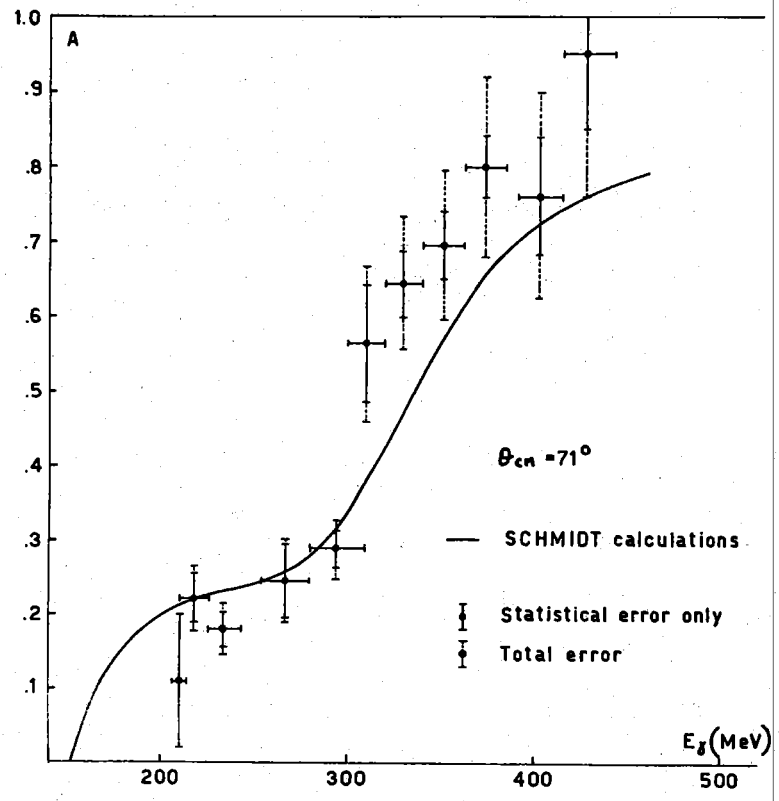

FIG. 12 c)

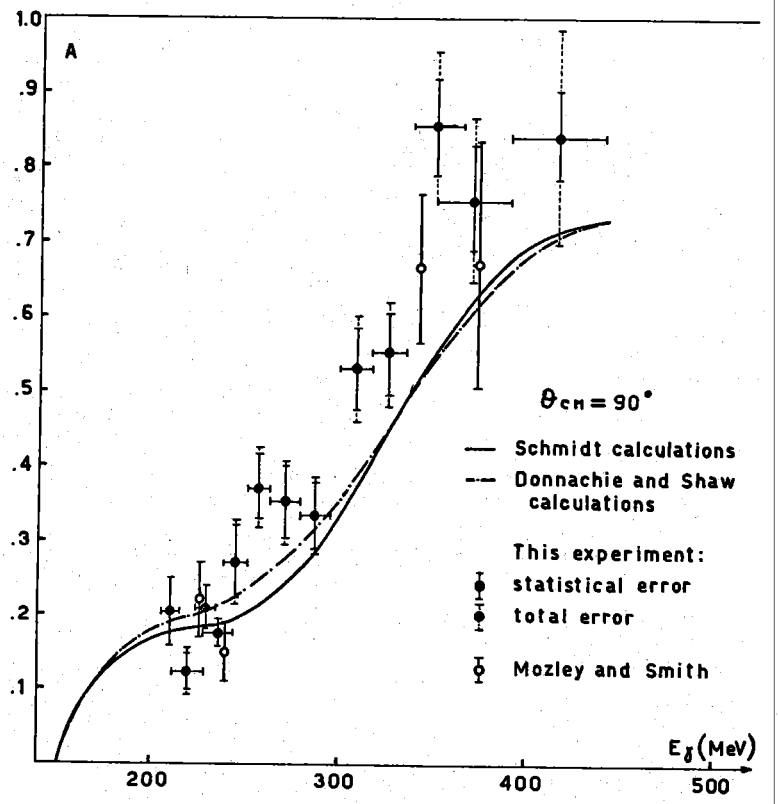

FIG. 12 d)

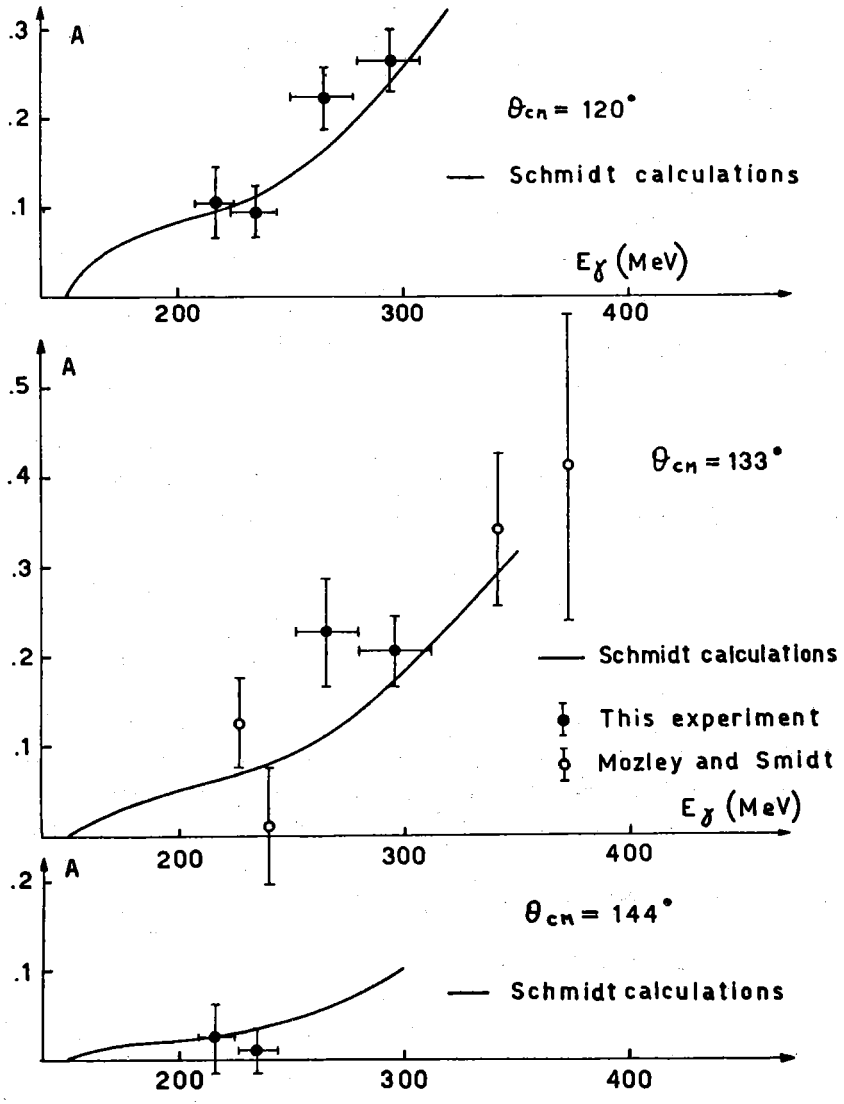

FIG. 12 e)

FIG. 12 (a, b, c, d, e) - Asymmetry ratio A vs E_γ for $\theta = 30^o; 45^o; 71^o; 90^o; 120^o; 133^o; 144^o$.

cannot be evaluated with sufficient accuracy starting from the present theories.

2) - Phenomenological analysis. -

As we have said in the introduction, from measurements of $A(\theta, E_\gamma)$ and from the photoproduction cross section (σ) by unpolarized gamma rays it is possible to determine separately $\sigma_\perp$ and $\sigma_{||}$

$$\begin{aligned} \sigma_\perp &= \sigma \cdot (1 + A(\theta, E_\gamma)) \\ \sigma_{||} &= \sigma \cdot (1 - A(\theta, E_\gamma)) \end{aligned} \tag{10}$$

The physical interest of this decomposition resides in the fact that in $\sigma_\perp$ we have no contribution from the "photoelectric term"(21), which introduces in the π^+ photoproduction waves with angular momentum $\ell > 1$ also near the threshold.

So the trasverse cross section, $\sigma_\perp$, may be analyzed, as the scattering cross section, in terms of few plane waves; e. e.

$$\sigma_\perp(\theta, E\ ) = \sum_{o}^{N} {}_n A_n (E_\gamma) \cos^n \theta \tag{11}$$

It is possible in this way to verify directly, if the photoproduction dynamics is similar to the scattering's one.

Moreover, from the angular coefficients A_n and from others coefficients, which can be obtained from the experimental data, we achieve sufficient equations to determine directly the multipole amplitudes.

3) - Comparison with the isobaric model(22). -

Some critical remarks have been put forward against the isobaric model(23) and its limitations.

Nevertheless, we are trying a comparison of our measurements of $\sigma_\perp$ with such a model in order to evaluate the transition amplitude γ-N-N^* (N = nucleon, N^* = (3/2, 3/2) nucleon isobars).

Numerical prediction of this amplitude has been made by means of the unitary simmetries(24), and by the quark model(25, 26). Moreover, the evaluation of this amplitude has some interest in connection with some recently proposed photoproduction sum rules(27, 28, 29) deduced from the current algebra.

REFERENCES. -

(1) - A. Donnachie and G. Shaw, Photopion production, dispersion relations and $\pi - \varrho - \gamma$ coupling, Dept. of Physics, University College, London; preprint (1965).
(2) - W. Schmidt, Z. Physik 182, 76 (1964).
(3) - G. T. Hoff, Phys. Rev. 122, 665 (1961).
(4) - M. Gourdin, Ph. Salin, Nuovo Cimento 27, 193 (1963).
(5) - R. C. Smith, R. F. Mozley, Phys. Rev. 130, 2429 (1963).
(6) - P. Gorenstein, M. Grilli, P. Spillantini, M. Nigro, E. Schiavuta, F. Soso and V. Valente, Phys. Letters 19, 157 (1965).
(7) - P. Gorenstein and al., Phys. Letters 23, 394 (1966).
(8) - H. Uberall, Phys. Rev. 103, 1055 (1956); 107, 223 (1957).
(9) - G. Barbiellini, G. Bologna, G. Diambrini and G. P. Murtas, Phys. Rev. Letters 8, 112 (1962).
(10) - G. Barbiellini, G. Bologna, G. Diambrini and G. P. Murtas, Phys. Rev. Letters 9, 9 (1962).
(11) - G. Barbiellini, G. Diambrini, F. Grianti, T. Letardi, G. P. Murtas, R. Visentin, Private communication.
(12) - G. Sacerdoti, L. Tau, Nucl. Instr. and Meth. 16, 139 (1962).
(13) - B. Borgia, P. Joos, M. Grilli, LNF 66/15 (1966).
(14) - D. Freytag, W. J. Schwille, R. J. Wedemeyer, Z. Physik 186, 1 (1965).
(15) - B. M. Chasan, G. Cocconi, V. T. Cocconi, R. M. Schectman, D. H. White, Phys. Rev. 119, 811 (1960).
(16) - M. Bloch, M. Sands, Phys. Rev. 113, 305 (1959).
(17) - A. Kusumegi, Y. Kobayashi, Y. Murata, H. Sasaki, K. Takamatsu, A. Masaike, Proceedings of the International Symposium on Electr. and photon Interactions, Hamburg (1965), vol. II, p. 253.
(18) - W. Schmidt, Proceedings of the International Symposium on Electr. and photon Interactions, Hamburg (1965), vol. II, p. 323.
(19) - W. Schmidt, H. Wunder, Phys. Letters 20, 541 (1966).
(20) - A. Donnachie, G. Show, Low Energy photopion production, SU(6) and the Panofsky ratio, CERN 66/749/5-TM. 673.
(21) - M. J. Moravcsik, Phys. Rev. 104, 1451 (1956).
(22) - Ph. Salin, Nuovo Cimento 28, 1294 (1963).
(23) - G. Höhler, Proceedings of the International Symposium on Electr. and photon Interactions, Hamburg (1965), vol. I, p. 55.
(24) - M. A. B. Bèg, B. W. Lee, A. Pais, Phys. Rev. Letters 13, 514 (1964).
(25) - R. H. Dalitz, Quark models for the "elementary particles" in high energy physics. Les Houches, (1965), p. 292.
(26) - R. Gatto, G. Veneziano, Phys. Letters 20, 439 (1966).
(27) - S. Fubini, C. Rossetti, F. Furlan, Nuovo Cimento 48 A, 161 (1966).
(28) - N. Mukunda, T. K. Radha, Equal time commutators and photoproduction sum rules, preprint Princeton University (1966).
(29) - S. L. Adler, F. J. Gilman, PCAC restrictions on pion photoproduction and electroproduction amplitudes, preprint (1966).
(30) - L. Criegee and al., Phys. Rev. Lett. 16, 1031 (1966).